AUT Journal of Civil Engineering

AUT J. Civil Eng., 6(2) (2022) 159-174
DOI: 10.22060/ajce.2022.19601.5742

Direct Design Method for RC Columns and Uniformly Reinforced Shear Walls based on Canadian Standards

J. Shafaei[1]*, R. Eskandari[2]

[1] Department of Civil Engineering, Shahrood University of Technology, Shahrood, Iran.
[2] Civil, Environmental and Land Management Engineering Department, Politecnico di Milano, Milan, Italy.

ABSTRACT: With a different attitude to conventional approaches and using curve and surface fitting, this paper proposes a straightforward Direct Design method for the design of eccentrically loaded RC columns and Uniformly Reinforced Shear Walls (URSWs) by which the longitudinal reinforcement ratio can be determined using the proposed equations and table. This method, which is proposed based on Canadian Standards Association (CSA 23.3-14) guidelines, is compatible with any applied axial load, moment, and cross-sectional dimensions which can decrease the graphical trial and error and be used in computer calculation and programming of RC structure. Several assessments on the effect of design parameters on the presentation manner of the proposed method have been carried out, and the validity and accuracy of the proposed method were investigated by comparison with conventional procedures. Averagely, there is a 3.48% difference between the required percentage of longitudinal reinforcement derived by the proposed method and design interaction diagrams. Also, the accuracy of all of the fitting processes carried out in this paper varies from 93.16% to 99% concerning the actual data points. It can be concluded that this method is suitable for a fast design of RC columns and URSWs with satisfying accuracy and validity.

Review History:

Received: Feb. 08, 2021
Revised: Feb. 28, 2022
Accepted: Nov. 12, 2022
Available Online: Nov. 30, 2022

Keywords:

Reinforced concrete structures
RC columns
P-M interaction diagrams
Curve fitting
Direct design method

1- Introduction

By assuming a series of strain distributions and computing the related values of axial and bending capacities in each distribution, Short Column Interaction Diagrams are derived. Using such diagrams along principal axes of symmetry is a common and accepted approach for the design of RC under combined axial load and bending moments [1].

The general procedure of designing RC columns and URSWs is defined as a series of iterations in which a cross-section is assumed, and the corresponding P-M (axial load-bending moment) interaction diagram (PMID) can be obtained. When the assumed cross-section satisfies the factored load and moment, which happens by falling applied [factored axial load, factored bending moment] point into the obtained PMID, then the iteration terminates. It means that the member with the assumed cross-section has adequate factored resistance (considering factored compressive strength of concrete and factored yield strength of steel) under the combination of factored axial load and moment [2]. Using interaction diagrams or other provided techniques may be confusing and time-consuming, which can be the reason for the increase in computational errors and decrease in accuracy, which is discussed in the next section. Any attempt at development in the design procedure without adding more computational cost and complexity can play an important role in structural design.

Several studies were carried out in an attempt to develop analysis and design aids and to propose different innovative procedures. Bresler [3] developed a reciprocal interaction equation used in ACI 318 commentary. Whitney [4] introduced an equivalent compression zone of the cross-section of RC members. Hsu [5] proposed a design aid relationship considering the nominal axial load and balanced axial load ratio. Fleming and Werner [6] developed design aids for columns subjected to biaxial bending. Nielsen [7] and Yen [8] introduced methods for the flexural capacity of cracked arbitrary concrete sections under axial load combined with biaxial bending. Bonet *et al.* [9] proposed an analytical approach for calculating failure surfaces in rectangular RC column cross-sections with symmetrical reinforcement. Paultre *et al.* [10] presented new equations for the design of confinement reinforcement for rectangular and circular columns. Barzegar and Erasito [11] developed interactive spreadsheets for concrete cross-section analysis under biaxial bending. Zenon *et al.* [12] introduced a method for designing RC short-tied columns using the optimization technique. Cedolin *et al.* [13] developed an approximate analytical solution for the failure envelope of rectangular RC columns. Mahamid and Houshiar [14] introduced a direct method and design diagrams for RC columns and shear walls. H. M. Afefy *et al.* [15] proposed a design procedure for braced RC columns with high-strength concrete, in which the columns

*Corresponding author's email: jshafaei@shahroodut.ac.ir

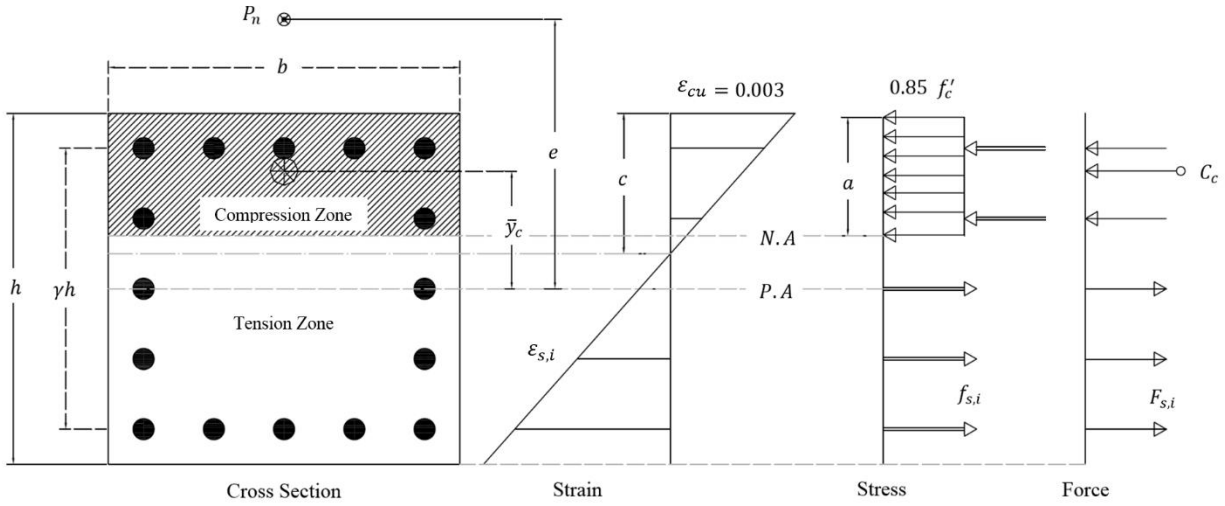

Fig. 1. Schematic representation of distribution theory for a column with a typical cross-section under eccentric loading.

are under uniaxial and biaxial compression. H. M. Afefy and ET.M EL-Tony [16] presented a simplified procedure for designing RC columns based on the equivalent column concept.

The characteristics of RC columns and their behavior under different loading conditions have been studied in recent decades. Chu and Pabarcius [17] studied the ultimate strength of biaxially loaded RC columns. Hsu and Mirza [18] studied adequate strength for biaxial bending and compression. Rodrigues *et al.* [19] studied the behavior of the RC column under biaxial cyclic loading. Lequesne-Pincheira [20] proposed revisions to the strength reduction factor for axially loaded members. Brondum- Wang-Hong [21] used the reciprocal load method for evaluating the capacity of RC columns of high-strength concrete.

Many researchers studied different shapes of the column and reported their design characteristics. Marin [22] developed design aids for L-Shaped RC columns. Hsu [23] presented theoretical and experimental results for biaxially loaded L-Shaped RC columns. Hsu [24] reported T-Shaped column behavior under biaxial bending and axial compression. Also, computer technology developments made researchers able to step into a different direction of RC column researches. Dinsmore [25] developed a program for column analysis with a programmable calculator. Ochoa [26] developed a computer algorithm for biaxial interaction diagrams for the short RC column of any cross-section.

Although the mentioned researchers presented several standpoints on the analysis and design of RC columns and studied different shapes of RC columns, by which several innovations were added to the field of study, more developments of such design methods to simplify the design process are of particular interest for professionals in structural engineering. Load capacity tables and using computer programs, as alternatives with sufficient accuracy and lower level of complexity rather than conventional approaches, are the other accepted procedures for RC column design [23].

This paper proposed an accurate, efficient, straightforward, Direct Design method that does not need computer programs and solves complicated differential equations. By the use of the proposed procedure, the longitudinal reinforcement area to cross-section gross area ratio (ρ) required in the design process of eccentrically loaded RC columns and URSWs can be directly calculated using proposed equations and tables in the method. The coefficients used in the proposed equations are listed in the tables and vary with the mechanical properties of concrete and steel (compressive strength of concrete ($f_c^{'}$) and yielding strength of steel (f_y)), the geometry of the cross-section (rectangular and circular cross-sections), and reinforcement arrangement (number of bars on each side and parameter γ). These six effective parameters in the design process are considered as design options in this approach, and their effect on the capacity of RC columns has been investigated in the next sections. The combination of these options is used to classify the final proposed tables and defined design cases presented in the tables. Due to being equation-based and universal, this method is distinguished from the others. Since the analysis used in the different stages of providing the final design equations is based on generally established theory, this method is accepted as an alternative design procedure for RC columns and URSWs [27]. Also, the effect of load and resistance safety factors are taken into account in the proposed method, so it should be noted that the safety level of the designed member using the proposed method corresponds to the safety level considered in CSA 23.3-14 standard.

2- Background

To achieve the goal of this paper, the modeling of the column is performed in MATLAB [28] based on the distribution theory, which is schematically shown in Fig. 1. Curve Fitting Application in MATLAB [28] also has been

used in determining the presented equations.

2- 1- Assumptions and modeling criteria

It should be noted that for deriving the PMID of a giving cross-section, the following three stages are performed for different values of c which is the distance from the fiber of maximum compressive strain to the neutral axis (N.A) (Nilson *et al.* [29]).

The longitudinal reinforcement is considered to be stress-perfect plastic, which means that the steel used for longitudinal reinforcement undergoes no work hardening after yield. The allowable interval for the percentage of longitudinal reinforcement in the cross-section is suggested to be $1\% \le \rho \le 8\%$ by CSA A23.3-14 [2].

2- 1- 1- Strain and stress distribution stage

The maximum strain at the extreme concrete compression fiber (ε_{cu}) is considered to be 0.003. The strain in the i th row of bars ($\varepsilon_{s,i}$) is defined as:

$$\varepsilon_{s,i} = \left[\frac{c - d_i}{c}\varepsilon_{cu}\right] \tag{1}$$

where d_i is the distance between i th row and fiber of maximum compressive strain. It is assumed that the trigonometric relationship is established between strains in the reinforcing bars and concrete. It should be noted that if the i th row of bars is placed at the compression zone, then $\varepsilon_{s,i}$ will be a positive value, and if the i th row of bars is situated at the tension zone, then $\varepsilon_{s,i}$ will be a negative value.

Since the tensile strength of concrete is approximately 10 to 15 percent of the compressive strength, the tensile strength of concrete is neglected. Also, the use of a stress block to replace an accurate approximation of concrete stress distribution is taken into consideration [2]. In the defined block, uniformly distributed concrete stress of $0.85f_c^{'}$ is assumed over an equivalent compressive region bounded by the edge of the cross-section and a straight line parallel to the neutral axis located a distance $a = \beta_1 c$ from the fiber of maximum compressive strain. The value of the coefficient β_1 is suggested to be $\beta_1 = 0.97 - 0.0025f_c^{'} \le 0.67$ [2]. The following equations calculate the created stress in the i th row of bars at the tension zone, the i th row of bars at the compression zone

$$\begin{cases} if\ \left|\varepsilon_{s,i}\right| < \varepsilon_{su} \rightarrow f_{s,i} = \varepsilon_{s,i}E_s \\ if\ \left|\varepsilon_{s,i}\right| \ge \varepsilon_{su} \rightarrow f_{s,i} = \phi_s f_y \end{cases} \tag{2}$$

where E_s and $\varnothing_s$ are the modulus of elasticity of steel which equals $2\times10^5\,MPa$ and resistance factor for steel whose value of 0.85 is suggested by CSA A23.3-14 [2], respectively.

2- 1- 2- Force calculation stage

After determining stress distribution, and considering $A_{s,i}$ as the total area of i th row of bars and A_c as the area of concrete in the compression zone, the force in each component of the cross-section is calculated as:

$$F_{s,i} = f_{s,i}A_{s,i} \tag{3}$$

$$C_c = 0.85\phi_c f_c^{'}A_c \tag{4}$$

where $F_{s,i}$, C_c and $\varnothing_c$ are a force in i th row of bars, compressive force in concrete, and the resistance factor for concrete, respectively.

In the square cross-sections, the area of compressive concrete is determined as:

$$A_c = a \times b \tag{5}$$

where b is the width of the cross-section. In the circular cross-sections, this parameter is specified as:

$$A_c = \frac{h_c}{4}(\theta - \sin\theta\cos\theta) \tag{6}$$

where θ in radian is

$$\begin{cases} \theta = \cos^{-1}\left(1 - \dfrac{2a}{h_c}\right) & for\ a \le \dfrac{h}{2} \\ \theta = 180° - \cos^{-1}\left(\dfrac{2a}{h_c} - 1\right) & for\ a > \dfrac{h}{2} \end{cases} \tag{7}$$

and h_c is the diameter of the circular cross-section.

2- 1- 3- Capacity calculation Stage

Finally, nominal compressive axial capacity (P_r), and the nominal flexural capacity of the column (M_r) are achieved according to the following relations:

$$P_r = C_c + \sum_{i=1}^{n} F_{s,i} \tag{8}$$

$$M_r = (C_c \bar{y}_c) + \sum_{i=1}^{n} (F_{s,i}\,\bar{y}_{s,i}) \tag{9}$$

where n, $\bar{y}_c$ and $\bar{y}_{s,i}$ are the number of bars on each

side, the distance between the centroid of the compressive zone of concrete and principal axis (P.A), and the distance between i th row of bars and P.A, respectively.

2- 2- Curve and surface fitting

Curve and Surface Fitting is a process of constructing a mathematical function that has the best fit to a given series of data points (Molugaram *et al.* [30] and McClarren *et al.* [31]). The precision of fit is evaluated based on four parameters including R-square (R^2), adjusted R-square, root mean square error (RMSE), and sum of squares due to error (SSE). A detailed discussion of these parameters is out of the beyond of this study. "Curve Fitting" is an application that is provided in MATLAB [28] and can fit appropriate curves in a 2-dimensional coordinate system and surfaces in the 3-dimensional coordinate system to the data points. To see more uses of this technique in different fields of research, refer to [32], [33], [34], [35], and [36].

3- Methodology

As discussed above, for reaching the desired PMID of a case of the cross-section with specific options including geometry, $f_c^{'}$, f_y, γ, and arrangement of bars, the three stages of the theory procedure have to be carried out for different values of c. Here, it is done for 300 values of c in the interval $[0, h^2/20]$ where h is the height of the cross-section, and this creates 300 loops of calculation in the modeling structure. Each one contains the theory procedure and the main idea of the study. All of the resultant points which fall into the fourth quarter of the derived PMIDs are neglected.

3- 1- Introduction of the main idea

According to the design aids provided by Nilson *et al.* [29], each slanted line cutting the curves of design diagrams shows a unique value of:

$$S = \frac{e}{h} \tag{10}$$

Where:

$$e = \frac{M_u}{P_u} \tag{11}$$

As can be figured out from the equations, e and S are the value of eccentricity and eccentricity to a height of the cross-section ratio, respectively. In this section of the paper, P and M are defined as nominal values to achieve eccentricity of the cross-section in each c. Since there is one unique point (M_n, P_n) for each c, there is one value of e for each c.

Two dimensionless parameters

$$W = \frac{P_u}{\phi_a f_c^{'} A_g} \tag{12}$$

$$Q = \frac{P_u e}{\phi_a f_c^{'} A_g h} \tag{13}$$

where W, Q and A_g are dimensionless axial capacity, dimensionless flexural capacity, and gross cross-sectional area ($A_g = b\,h$ for the square section and $A_g = \pi h_c^2/4$ for circular section), respectively, establish the design diagrams. In this paper, two parameters of W and S are considered significant parameters. In other words, the presented equations for determining the percentage of longitudinal reinforcement in the cross-section are two-variable functions of W and S.

Since the column behavior is assessed in each integer percentage of ρ, 1% to 8%, the diameter of bars D considered in rectangular cross-section is derived as:

$$D = \sqrt{\frac{4\rho A_g}{\pi n_b}} \tag{14}$$

where n_b is the total number of bars in the cross-section. After determining P_r and M_r of each ρ of any case for 300 c, W, and S are easily computed. Fig. 2 illustrates the fundamental steps of transposing the diagrams for a case with $h = b = 50cm$, $f_c^{'} = 28MPa$, $f_y = 420MPa$, $\gamma = 0.8$, $\rho = 4\%$, and 5 bars at each side.

3- 2- Fitting process

After determining 600 values of each desired dimensionless parameter, W, and S, for eight ρ in each case and then neglecting negative values, the fitting process has to be applied to the data series. A 2D fitting is used to establish the equation $W = f(S)$ for each ρ.

3- 2- 1- Formulation in curve fitting

There are different built-in types of 2D fitting available in the curve fitting application provided in MATLAB [28], which can be selected for the fitting process by the user according to the behavior of the data set of points. Each built-in type uses a unique mathematical model. Also, there is a custom type in which the mathematical model can be applied manually. It is evident that each mathematical model, either built-in or manually applied, shows unique precision of fit in the fitting process. The type of 2D fitting used in this paper is a built-in type named Rational in which the numerator degree and denominator degree are selected 2 and 3, respectively. The general mathematical model used in this type is defined as:

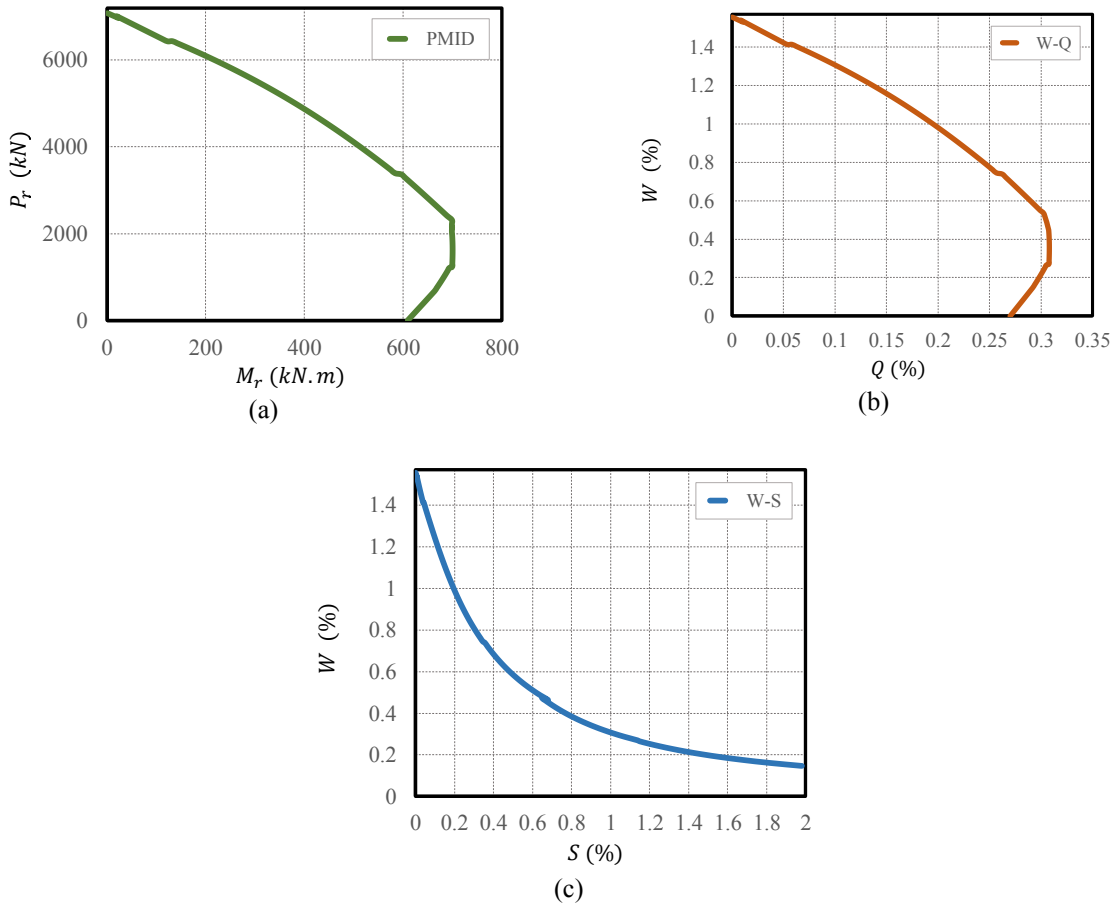

Fig. 2. Stepwise graphical process of transposing diagrams from (a) PMID to (b) W-Q interaction diagram and then to (c) W-S diagram for a cross-section with h=b=50 cm, $f_c^{'}$ =28 *MPa* , f_y= 420 MPa, γ=0.8 and 5 bars on each side (ρ=4%)

$$f(x)=\frac{p_1x^2+p_2x+p_3}{x^3+q_1x^2+q_2x+q_3} \tag{15}$$

where p_1 to p_3 and q_1 to q_3 are the coefficients whose determination is the main objective of this fitting process. It should be noted that $f(x)$ and x are related to W and S , respectively. It is useful to mention that the highest power of x is 2 in the numerator (numerator degree) and 3 in the denominator (denominator degree). As the 2D fitting is carried out only for initializing data for 3D fitting, the number of coefficients does not play an important role in the simplicity of the proposed method. But the values which describe the precision of fitting are considerable because they affect the final accuracy of the method. Fig. 3(a) shows the data points and fitted curve for $\rho=4\%$ of a case with a rectangular cross-section, $f_c^{'}=28MPa$, $f_y=420MPa$, $\gamma=0.8$, and 5 bars on each side. By doing this for eight ρ of a case, WS diagram of this case is derived, which is shown in Fig. 3(b). To represent the accuracy of the fitting process, the values specifying the precision of fit for each ρ of this case are listed in Table 1. When the value of R^2 which varies in the interval $[-\infty,1]$ is obtained equal to 1 in the fitting process, which means that the curve or surface is perfectly fitted to the data set of points.

3- 2- 2- Formulation in surface fitting

To present the main equation $\rho=f(W,S)$, a series of data points is needed. After applying 40 points in the interval [0,2] of S at the $W=f(S)$ for every eight ρ , which is derived from the 2D fitting, the data points for eight ρ on each case are available. These sets of data are used for 3D fitting in which a Polynomial type of fitting is considered.

The selection of the mathematical model for formulation used in this paper is carried out according to (1) fewer coefficients to make the design procedure simpler, (2) higher R^2 to improve the accuracy of the method. As the built-in types of 3D fitting do not show an adequate behavior to the data set of points due to their unique mathematical model,

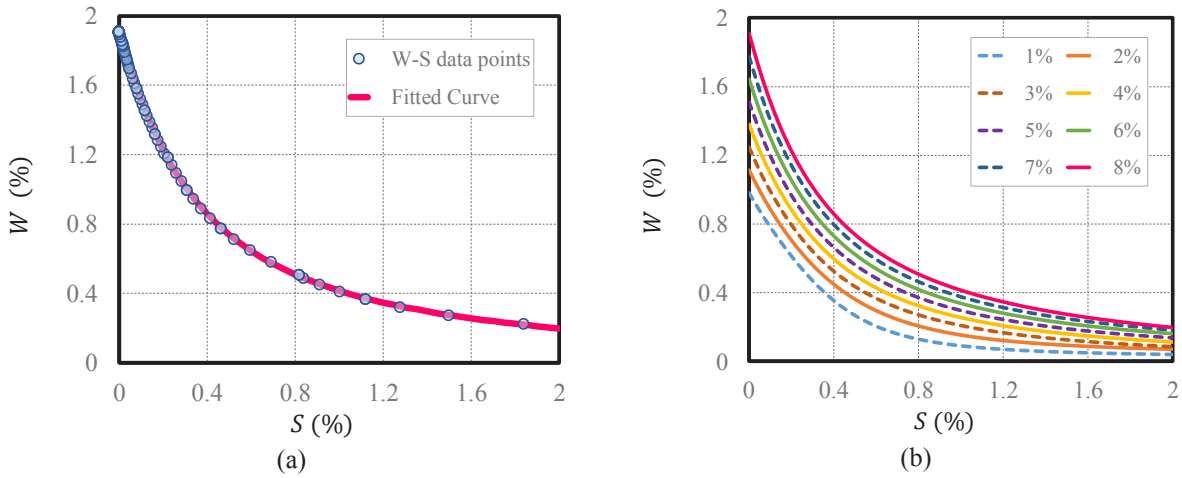

Fig. 3. a) Data points and fitted W-S curve for ρ=8%, and (b) fitted W-S curves for eight ρ of a case with a rectangular cross-section, $f_c^{'} = 28\ MPa$, f_y= 420 MPa, γ=0.8 and 4 bars on each side

Table 1. The precision of fitting performed in Fig. 8(b)

	Values of ρ							
Precision of fit	**1%**	**2%**	**3%**	**4%**	**5%**	**6%**	**7%**	**8%**
R^2	1	1	1	1	1	1	1	1
RMSE	0.00097	0.00115	0.001341	0.001516	0.001757	0.001886	0.002072	0.002273

Table 2. A comparison between the best possible models for obtaining ρ in rectangular cross-sections.

Mathematical Model of $f(x,y)$	Num. of Coefficients	R^2	*RMSE*
$u_1 + u_2x + u_3xy$	3	0.6791	0.01304
$u_1 + u_2y + u_3xy$	3	0.8230	0.00968
$u_1 + u_2x^2 + u_3xy$	3	0.6701	0.01322
$u_1 + u_2y^2 + u_3xy$	3	0.9083	0.00697
$u_1 + u_2x^2 + u_3y + u_4xy$	4	0.8989	0.00733
$u_1 + u_2x + u_3y^2 + u_4xy$	4	0.9722	0.00385
$u_1 + u_2x + u_3x^2 + u_4y^2 + u_5xy$	5	0.9851	0.00282
$u_1 + u_2x^2 + u_3y + u_4y^2 + u_5xy$	5	0.9800	0.00326

a numerical comparison among the best possible custom (manually applied) mathematical models is provided in Table 2 for rectangular cross-section and Table 3 for the circular cross-section. Also, the value of RMSE for each model is listed in the tables for more information. This comparison is performed for a case with $f_c^{'} = 28 MPa$, $f_y = 420 MPa$, $\gamma = 0.8$, and 4 bars on each side for the rectangular cross-section and eight total bars on the circular cross-section. According to Table 2, the model with four coefficients and a value of 0.9900 for R^2 is achieved which benefits from the best R^2 value and relatively fewer coefficients among others. Also, the model with five coefficients and a value of

Table 3. A comparison between the best possible models for obtaining ρ in circular cross-sections.

Mathematical Model of $f(x,y)$	Num. of Coefficients	R^2	*RMSE*
$u_1+u_2x+u_3xy$	3	0.6791	0.01304
$u_1+u_2y+u_3xy$	3	0.8230	0.00968
$u_1+u_2x^2+u_3xy$	3	0.6701	0.01322
$u_1+u_2y^2+u_3xy$	3	0.9083	0.00697
$u_1+u_2x^2+u_3y+u_4xy$	4	0.8989	0.00733
$u_1+u_2x+u_3y^2+u_4xy$	4	0.9722	0.00385
$u_1+u_2x+u_3x^2+u_4y^2+u_5xy$	5	0.9851	0.00282
$u_1+u_2x^2+u_3y+u_4y^2+u_5xy$	5	0.9800	0.00326

Table 4. Results of the surface fitting shown in Fig. 9

u_1	u_2	u_3	u_4	R^2
-2.308	0.8088	3.114	21.2	0.9900

0.9851 for R^2 shows the best results to be considered as a suitable model for formulation.

So, Eqs. (16) and (17) show the general mathematical models which are defined for cases with a rectangular and circular cross-section, respectively.

$$f(x,y)=u_1+u_2x+u_3y^2+u_4xy \quad (16)$$

$$f(x,y)=u_1+u_2x+u_3y^2+u_4y^2+u_5xy \quad (17)$$

where the coefficients u_1 to u_5 are the main objectives that should be calculated. The variables x , y, and $f(x,y)$ represent S , W , and ρ , respectively.

The 3D visualization of the data points and the final fitted surface are shown in Fig. 4. Finally, the results of the fitting shown in Fig. 9 are listed in Table 4. It is essential to mention that the output of the proposed equation for ρ is calculated in percentage so that this obtained value has to be divided by 100.

4- Sensitivity of the Model to Options

As can be realized from the conventional design diagrams, the dimension option is neglected in the list of options for each case, because the axial capacity is divided by the dimension of the cross-section. It means that these diagrams apply to any desired dimensions. But, despite dividing the capacity by f_c' in dimensionless axial capacity, f_c' remains as an option in each case. Therefore, a detailed practical evaluation of the effectiveness of each option on capacity values can be useful, which is carried out in this section. This assessment is carried out by comparison of W-Q interaction diagrams. Any effect on this diagram is similar to the W-S diagram, which is the basis of the method. Since the cross-section geometry is an inevitable fixed option for a case, the effect of this option is not evaluated in this section.

4- 1- Cross-sectional dimensions

Fig. 5(a) shows the W-Q diagrams for two cross-sections with rectangular geometry and dimensions of $h=40cm$ and $b=50cm$ and square geometry and dimensions of $h=b=100cm$, assuming $f_c'=28MPa$, $f_y=420MPa$, $\gamma=0.8$, $\rho=4\%$, and 5 bars on each side. The perfect match between the data series of two cross-sections shows that eliminating the dimension option from each case is reasonable. Also, this is shown that this method is suitable for designing both RC columns and URSWs with different dimensions. It can help the generalization of the method by which the value of ρ can be determined for any desired dimension. It is useful to mention that the geometry of the column, which is considered as a lateral option in each case, is latent in the dimension option. In this paper, dimensions of $h=b=50cm$ and $h=b=200cm$ are simultaneously

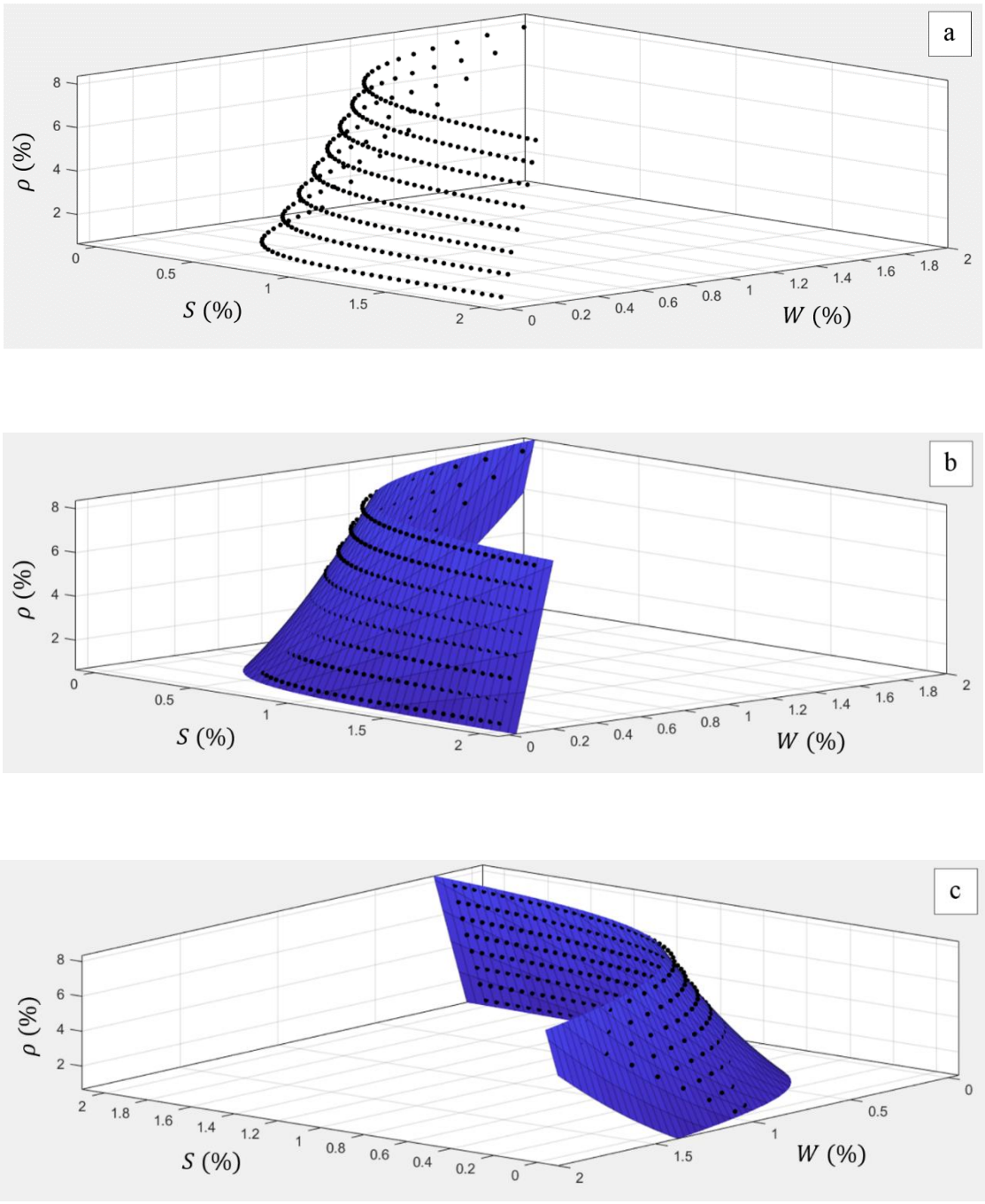

Fig. 4. 3D visualization of (a) data points, (b) view1 of fitted surface, and (c) view2 of fitted surface, according to the selected general model of obtaining ρ, for a case with rectangular cross-section, $f_c^{'} = 28\ MPa$, f_y= 420 MPa, γ=0.8 and 4 bars on each side

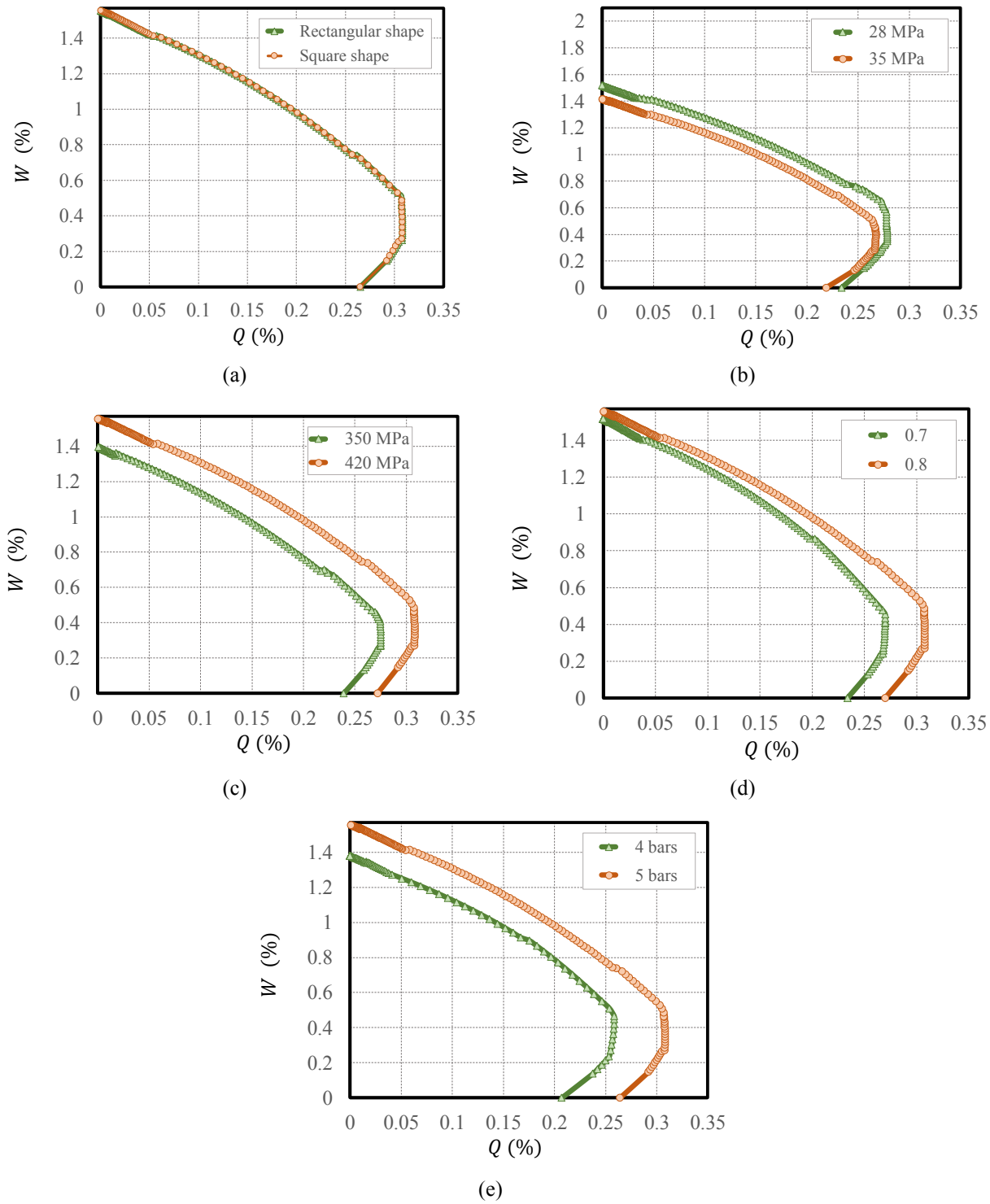

Fig. 5. Effect of (a) Cross-sectional dimensions, (b) $f_c^{'}$, (c) f_y, (d) Parameter γ, and (e) Arrangement of Bars on W-Q diagram.

Table 5. Direct design method for rectangular cross-section and 4 bars on each side.

Short RC Columns and Uniformly Reinforced Shear Walls • Rectangular Cross-section • 4 Bars on Each Side of Cross-section								
Case	**Option** f'_c **and** f_y **in MPa**			$\rho^{rectangular} = u_1 + u_2 S + u_3 W^2 + u_4 S\,W$ $e = \frac{M_u}{P_u}$, $S = \frac{e}{h}$, $W = \frac{P_u}{\emptyset f_y A_g}$				
	f'_c	f_y	γ	u_1	u_2	u_3	u_4	R^2
1	28	420	0.6	-2.558	0.7818	3.488	29.31	0.9676
2	28	420	0.7	-2.187	0.4749	3.156	25.00	0.9661
3	28	420	0.8	-2.308	0.8088	3.114	21.20	0.9900
4	28	420	0.9	-1.953	0.6385	2.817	18.01	0.9886
5	35	420	0.6	-2.460	0.6543	3.996	33.20	0.9377
6	35	420	0.7	-3.017	1.1860	4.239	29.58	0.9789
7	35	420	0.8	-2.674	1.0340	3.911	25.13	0.9828
8	35	420	0.9	-2.438	0.9443	3.655	21.56	0.9883

studied for each case for more assurance.

4- 2- Compressive strength of concrete

The parameters $h = b = 50cm$, $f_y = 420MPa$, $\gamma = 0.8$, $\rho = 4\%$, and the arrangement of 5 bars on each side is considered for $f_c^{'} = 28MPa$ and $f_c^{'} = 35MPa$ in this section. The curve related to $f_c^{'} = 28MPa$ is shifted to the right, which means that the cross-section with $f_c^{'} = 28MPa$ benefits from more dimensionless capacity, when compared to the cross-section with $f_c^{'} = 35MPa$ (see Fig. 5(b)). So, this mismatch between the two curves is a reason for considering this parameter as an option in the method.

4- 3- Tensile strength of steel

Since f_y does not cooperate in the task of dividing the capacity, this parameter cannot be dismissed from the list of options of a case. The interaction diagrams of a cross-section with $h = b = 50cm$, $f_c^{'} = 28MPa$, $\gamma = 0.8$, $\rho = 4\%$ and arrangement of 5 bars on each side for $f_y = 350MPa$ and $f_y = 420MPa$ are displayed in Fig. 5(c), which is graphical proof to this fact. In contrast with the $f_c^{'}$ option, the cross-section with higher yielding strength of steel ($f_y = 420MPa$) shows an increase in dimensionless capacity.

4- 4- Parameter γ

The behavior of two cross-sections with $h = b = 50cm$, $f_c^{'} = 28MPa$, $f_y = 420MPa$, $\rho = 4\%$, and 5 bars on each side for $\gamma = 0.7$ and $\gamma = 0.8$ is illustrated in Fig. 5(d). As can be seen in the figure, the distance between the two curves increases from the compression zone to the tension zone. In other words, the effect of this parameter on the capacity of the cross-section is more intense in the tension zone. Therefore, this parameter remains an option in each case.

4- 5- Arrangement of bars

The mismatch between the two diagrams illustrated in Fig. 5(e) which is corresponded to a cross-section with $h = b = 50cm$, $f_c^{'} = 28MPa$, $f_y = 420MPa$, $\gamma = 0.8$, $\rho = 4\%$ for two arrangements of 4 and 5 bars on each side shows that the option of bars arrangement cannot be deleted from the list of options of a case. This figure shows the most extreme mismatch among the other figures, which relate to the effectiveness of the design parameter, and also specifies the importance of this parameter in the capacity of cross-section, which is neglected in the design diagrams presented in the design aids such as [37]. In this design aid, the number of bars on each side is not listed as an option for provided design diagrams, but an equal number of bars on all of the faces is considered as the criteria related to the arrangement of bars in the cross-section.

5- Results and Discussion

The described procedure for proposing the Direct Design method is carried out for different cases with commonly used options. The final proposed tables and equations used in the Direct Design method are provided in Tables 5 to 7 The considered mathematical models which are compatible with all of the cases in the corresponding table are provided. Instead of using design diagrams, these tables of this method can be used for the design of eccentrically loaded columns and URSWs.

For a given factored load P_u and factored bending moment M_u , the following steps are proposed for designing columns and URSWs:

Calculate eccentricity $e = M_u / P_u$.

Select cross-sectional dimensions b and h for URSWs and rectangular, or h_c for the circular cross-section.

Table 6. Direct Design method for Rectangular cross-section and 5 bars on each side.

Short RC Columns and Uniformly Reinforced Shear Walls
- Rectangular Cross-section
- 5 Bars on Each Side of Cross-section

Case	Option f'_c and f_y in MPa			$\rho^{rectangular} = u_1 + u_2 S + u_3 W^2 + u_4 S\,W$ $e = \frac{M_u}{P_u}$, $S = \frac{e}{h}$, $W = \frac{P_u}{\emptyset f_y A_g}$				
	f'_c	f_y	γ	u_1	u_2	u_3	u_4	R^2
1	28	420	0.6	-2.101	0.4621	2.527	24.36	0.9790
2	28	420	0.7	-1.776	0.3583	2.304	19.97	0.9863
3	28	420	0.8	-1.547	0.2818	2.104	16.86	0.9890
4	28	420	0.9	-1.304	0.2398	1.922	14.18	0.9893
5	35	420	0.6	-2.367	0.4099	3.171	29.02	0.9608
6	35	420	0.7	-2.217	0.6778	3.038	23.64	0.9810
7	35	420	0.8	-2.056	0.6382	2.831	20.19	0.9854
8	35	420	0.9	-1.672	0.4486	2.553	17.05	0.9870

Table 7. Direct design method for Circular cross-section and 8 total bars on the cross-section.

Short RC Columns
- Circular Cross-section
- 8 total Bars on Cross-section

Case	Option f'_c and f_y in MPa			$\rho^{circular} = u_1 + u_2 S + u_3 S^2 + u_4 W^2 + u_5 SW$ $e = \frac{M_u}{P_u}$, $S = \frac{e}{h}$, $W = \frac{P_u}{\emptyset f_y A_g}$					
	f'_c	f_y	γ	u_1	u_2	u_3	u_4	u_5	R^2
1	28	420	0.6	-4.346	4.333	-1.739	4.840	48.38	0.9316
2	28	420	0.7	-5.047	4.483	-1.602	5.181	47.66	0.9646
3	28	420	0.8	-4.669	3.834	-1.138	5.030	42.11	0.9851
4	28	420	0.9	-4.159	4.483	-1.650	4.869	34.82	0.9761
5	35	420	0.6	-5.697	5.986	-2.265	6.442	57.84	0.9353
6	35	420	0.7	-5.464	6.355	-2.444	6.422	50.13	0.9503
7	35	420	0.8	-5.991	6.349	-2.243	6.726	49.10	0.9666
8	35	420	0.9	-5.378	5.288	-1.660	6.377	43.69	0.9782

Calculate $S = e / h$ and $W = P_u / \varnothing_c f_c^{'} A_g$.

Calculate $\rho = f(S, W)$ according to the corresponding table.

Calculate the total longitudinal steel longitudinal reinforcement area $A_{st} = \rho bh / 100$.

According to the effectiveness assessments (see Section 4), the proposed values in these tables are only applicable to mentioned corresponding options. Fig. 6 shows the flowchart of the overall process of obtaining the equations and corresponding coefficients for designing RC columns and URSWs, which can be used for deriving this information for other options which are not provided in this study.

6- Method Validation and Accuracy

As discussed in Section 2, it is obvious that the Direct Design method can make the design process faster and also can provide more accurate results using provided equations and tables in comparison with other methods, but it is crucial to assess the accuracy of the method and validate the method. The validation is carried out through an example in which the results derived by the proposed method are compared to the results of the other method, i.e., using design interaction diagrams.

6- 1- Method accuracy

The value of R^2, which is the main component of the precision of fitting parameters, was used to evaluate the accuracy of the method. Table 8 presents a brief assessment of three proposed tables according to R^2 values. It is clear from this table that the best results are achieved for case 3 of Table 5, which corresponds to the rectangular cross-section with 4 bars at each side. This case has a minimum error of 1%, and the maximum error of 8.84% relates to case 1 of Table 8 with $R^2 = 0.9116$.

6- 2- Examples

A cross-section with properties of $f_c^{'} = 35\,MPa$ (5 ksi), $f_y = 420\,MPa$ (60 ksi), $\gamma = 0.8$ which is subjected to $P_u = 3200$ kN (719.3 kips) and $M_u = 480$ kN.m (353.7 kips. ft) is assumed. Calculate the value of ρ for commonly used dimensions of 1) square cross-section with 4 bars at each side (see Fig. 1, assuming $h = b$ and only 4 bars at each side), 2) circular cross-section with a total of 8 bars, and 3) rectangular cross-section of URSW with 5 bars at each side (see Fig. 1, same bars arrangement and assuming $h = 3m$).

6- 2- 1- Solutions

First of all, $e = 0.15$ m. Using the mentioned steps and Case 7 in Tables 6 to 8 for examples 1 to 3, respectively, the solution continues in Table 9. Also, the results from the design interaction diagrams based on visual inspections are provided to make a comparison of two procedures, i.e., the proposed Direct Design method and design interaction diagrams presented in Pillai and Kirk [37]. This reference provides design interaction diagrams based on the specifications and guidelines of CSA 23.3-14. Since the visual inspection is used for obtaining results from design interaction diagrams,

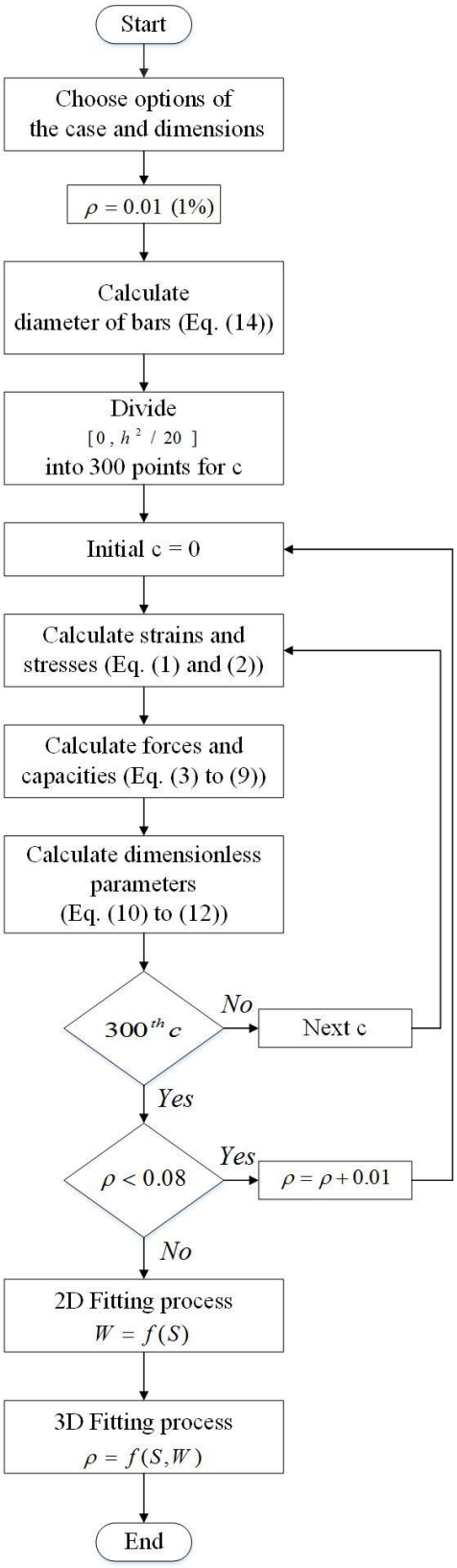

Fig. 6. Flowchart of the overall process of deriving equations and corresponding coefficients.

Table 8. Evaluation of method accuracy according to R^2 values.

	Table 6		Table 7		Table 8		All tables	
	Mean Value	Maximum	Mean Value	Maximum	Mean Value	Maximum	Mean Value	Maximum
R^2 value	0.9750	0.9900	0.9822	0.9893	0.9585	0.9851	0.9719	0.9900
Case Number	-	3	-	4	-	3	-	3 (Table 6)

Table 9. Values of ρ derived using the Direct Design method and design interaction diagrams presented in [37].

Geometry of Cross-section	Dimensions [cm] ([in])	S [%]	W [%]	Direct Design Method	Design interaction diagram [37]
				ρ [%]	ρ [%]
1) Square	45×45 (17.7×17.7)	0.3333	0.6946	5.3754	≈ 5.40
	50×50 (19.7×19.7)	0.3000	0.5629	2.5404	≈ 2.50
	55×55 (21.7×21.7)	0.2727	0.4649	1.6392	≈ 1.50
2) Circular	55 (21.7)	0.2727	0.5923	5.8638	≈ 5.40
	60 (23.6)	0.2500	0.4977	3.2314	≈ 3.10
	65 (25.6)	0.2308	0.4241	1.3689	≈ 1.30
3) Rectangular (URSW)	20×300 (7.9×118.1)	0.7500	0.2344	2.1276	≈ 2.20
	23×300 (9.1×118.1)	0.6521	0.2039	1.1624	≈ 1.30
	25×300 (9.8×118.1)	0.6000	0.1875	0.6975	≈ 0.70

approximate values of ρ are determined. An acceptable amount of difference is seen between ρ derived by the proposed method and the corresponding ρ calculated based on Pillai and Kirk [37]. So, the results obtained based on the design interaction diagrams of Pillai and Kirk [37] seem to be suitable benchmarks for comparison and validation. The average percentage of differences between the results of the proposed method and design diagrams presented by Pillai and Kirk [37] is 3.48%, which shows that the proposed method benefits from adequate validity to be used for designing RC columns and URSWs.

7- Conclusion

In this paper, using the 3D fitting process, a straightforward equation-based Design method is proposed by which the values of ρ in the design process of RC columns and URSWs can be calculated. The proposed design tables are applicable for common values of mechanical properties and bars arrangement in RC columns' cross-section. The comparison between the required reinforcement ratios obtained according to the proposed approach and conventional methods provided by Canadian Code, for assumed cross-sectional properties and applied loads, shows a reasonable and satisfactory small difference (average of 3.48% error), which is on the safe side in the case of Square and Circular cross-sections. The concluded key points according to the work carried out in this paper can be summarized as follows.

Direct Design method is applicable for designing columns and uniformly reinforced shear walls with any desired dimensions.

The derived value of ρ by this method is the exact required amount in the design process.

The Direct Design method permits faster and more accurate results.

The options, including the geometry of the cross-section, the arrangement of bars, f_c', f_y and parameter γ cannot be neglected from the list of options of proposed tables.

The idea of using the fitting technique is responsive to the final goal of this paper and can be used for generating more information for any required option.

The effect of slenderness is not considered in this method and may be considered in a future study.

References

[1] J.K. Wight, J.G. Macgregor, Reinforced Concrete Mechanics and Design, 2012, in, Pearson Education, Inc., Upper Saddle River, New Jersey.

[2] Canadian Standards Association Group, 2014. Design of concrete structures (CSA A23.3-14). Mississauga, Ontario, Canada L4W 5N6, 61-75.

[3] B. Bresler, Design criteria for reinforced columns under axial load and biaxial bending, in: Acids J. Proc., 1960, 481-490.

[4] C.S. Whitney, Plastic theory of reinforced concrete design, Transactions of the American Society of Civil Engineers, 107(1) (1942) 251-282.

[5] C.-T.T. Hsu, Analysis and design of square and rectangular columns by equation of failure surface, Structural Journal, 85(2) (1988) 167-179.

[6] J.F. Fleming, S.D. Werner, Design of columns subjected to biaxial bending, in, 1965, pp. 327-342.

[7] T. Brondum-Nielson, Ultimate Flexural Capacity of Partially or Fully Prestressed Cracked Arbitrary Concrete Sections under Axial Load Combined with biaxial bending, Concrete International, 5(1) (1983) 75-78.

[8] J.Y.R. Yen, Quasi-Newton method for reinforced-concrete column analysis and design, Journal of Structural Engineering, 117(3) (1991) 657-666.

[9] J.L. Bonet, P.F. Miguel, M.A. Fernandez, M.L. Romero, Analytical approach to failure surfaces in reinforced concrete sections subjected to axial loads and biaxial bending, Journal of Structural Engineering, 130(12) (2004) 2006-2015.

[10] P. Paultre, F. Légeron, Confinement reinforcement design for reinforced concrete columns, Journal of structural engineering, 134(5) (2008) 738-749.

[11] F. Barzegar, T. Erasito, Concrete sections under biaxial bending: Interactive analysis with spreadsheets, Concrete International, 17(12) (1995) 28-33.

[12] Z.A. Zielinski, W. Long, M.S. Troitsky, Designing reinforced concrete short-tied columns using the optimization technique, Structural Journal, 92(5) (1995) 619-626.

[13] L. Cedolin, G. Cusatis, S. Eccheli, M. Roveda, Biaxial bending of concrete columns: an analytical solution, Studies and researches, 26 (2006).

[14] M. Mahamid, M. Houshiar, Direct Design method and design diagrams for reinforced concrete columns and shear walls, Journal of Building Engineering, 18 (2018) 66-75.

[15] H.M. Afefy, S.F. Taher, S.E. El-Metwally, A new design procedure for braced reinforced high strength concrete columns under uniaxial and biaxial compression, Arabian Journal for Science and Engineering, KFUPM, KSA, 34 (2009) 349-377.

[16] H.M. Afefy, E.-T.M. El-Tony, Simplified design procedure for reinforced concrete columns based on equivalent column concept, International Journal of Concrete Structures and Materials, 10(3) (2016) 393-406.

[17] K.H. Chu, A. Pabarcius, Biaxially loaded reinforced concrete columns. J. Struct. Div. ASCE, 84(ST8) (1958), 1-27.

[18] C.-T. Hsu, M.S. Mirza, Structural concrete-biaxial bending and compression, Journal of the Structural Division, 99(2) (1973) 285-290.

[19] H. Rodrigues, H. Varum, A. Arêde, A.G. Costa, Behaviour of reinforced concrete column under biaxial cyclic loading—state of the art, International Journal of Advanced Structural Engineering, 5(1) (2013) 1-12.

[20] R.D. Lequesne, J.A. Pincheira, Proposed revisions to the strength-reduction factor for axially loaded members, in, American Concrete Institute, 2014.

[21] W. Wang, H.P. Hong, Appraisal of reciprocal load method for reinforced concrete columns of normal and high strength concrete, Journal of Structural Engineering, 128(11) (2002) 1480-1486.

[22] J. Marin, Design aids for L-shaped reinforced concrete columns, in, 1979, pp. 1197-1216.

[23] C.-T.T. Wsu, Biaxially loaded L-shaped reinforced concrete columns, Journal of structural engineering, 111(12) (1985) 2576-2595.

[24] C.-T.T. Hsu, T-shaped reinforced concrete members under biaxial bending and axial compression, Structural Journal, 86(4) (1989) 460-468.

[25] C.I. Dinsmore, Column analysis with a programmable calculator, Concrete International, 4(11) (1982) 32-36.

[26] J.A. Rodriguez, J.D. Aristizabal-Ochoa, Biaxial interaction diagrams for short RC columns of any cross-section, Journal of Structural Engineering, 125(6) (1999) 672-683.

[27] Canadian Standards Association Group, 2014. Design of concrete structures (CSA A23.3-14). Mississauga, Ontario, Canada L4W 5N6, 18-20.

[28] MATLAB and Statistics Toolbox Release 2018b. MathWorks, Inc., Natick, Massachusetts, U.S.

[29] A.H. Nilson, G. Winter, Design of Concrete Structures, Tenth Ed., in, McGraw-Hill, Inc., New York, 1987.

[30] K. Molugaram, G.S. Rao, A. Shah, N. Davergave, Statistical techniques for transportation engineering, Butterworth-Heinemann, 2017.

[31] R. McClarren, Computational nuclear engineering and radiological science using python, Academic Press, 2017.

[32] B. Elsener, O. Klinghoffer, T. Frolund, E. Rislund, Y. Schiegg, H. Böhni, Assessment of reinforcement corrosion by means of galvanostatic pulse technique, in, 1997, pp. 391-400.

[33] R.B. Polder, M.R. De Rooij, Durability of marine concrete structures: field investigations and modeling, Heron, 50 (3), (2005).

[34] R. Heiyantuduwa, M.G. Alexander, Studies on prediction models for concrete durability, in: Concrete Repair, Rehabilitation and Retrofitting II, CRC Press, 2008, pp. 165-166.

[35] Z. Li, Z. Peng, J. Teng, Y. Wang, Experimental study of damage evolution in circular stirrup-confined concrete, Materials, 9(4) (2016) 278.

[36] M. Hasan, A. Kabir, Early age tests to predict 28 days compressive strength of concrete, Caspian Journal of Applied Sciences Research, 2 (2013) 234-241.

[37] S.U. Pillai, D.W. Kirk, Reinforced Concrete Design, in, McGraw-Hill Inc., Ryerson, New York, 1988.

Nomenclature

a	height of the stress block of the concrete compression zone
A_c	area of the concrete compression zone
A_g	cross-section gross area
b	width of cross-section
c	distance from the fiber of maximum compressive strain to the neutral axis
C_c	force in the concrete compression zone
d_i	distance from the fiber of maximum compressive strain to the centroid of ith row of bars
D	diameter of bar
e	eccentricity
E_s	elastic modulus of steel
f_c'	compressive strength of concrete
$f_{s,i}$	stress in ith row of bars
$F_{s,i}$	force in ith row of bars
f_y	yield strength of steel
h	height of cross-section
h_c	diameter of circular cross-section
M_u	factored bending moment
M_r	nominal flexural capacity
N.A	neutral axis
n_b	total number of bars at the cross-section
P.A	principal axis
$p_1, .., p_3$	coefficients of the numerator in 2Dfitting
P_u	factored axial load
P_r	nominal axial capacity
$q_1, .., q_3$	coefficients of the denominator in 2Dfitting
Q	dimensionless flexural capacity
R^2	R-squared value in the precision of fit
S	eccentricity to the height of the cross-section
$u_1, .., u_5$	coefficient of polynomial 3D fitting
W	dimensionless axial capacity
$\bar{y}_c$	distance from the centroid of the concrete compression zone to the principal axis
$\bar{y}_{s,i}$	distance between ith row of bars and principal axis
γ	distance between the first and last row of bars to the height of cross-section ratio
$\emptyset$	strength reduction factor
ρ	reinforcement area to cross-section gross area ratio
θ	angle in a circular cross-section which determines the compression zone
ε_{cu}	the maximum compressive strain of concrete
$\varepsilon_{s,i}$	strain in ith row of bars

HOW TO CITE THIS ARTICLE
J. Shafaei, R. Eskandari, Direct Design Method for RC Columns and Uniformly Reinforced Shear Walls based on Canadian Standards, AUT J. Civil Eng., 6(2) (2022) 159-174.

DOI: 10.22060/ajce.2022.19601.5742